

Simulation Techniques and Control Schemes in Electromyography for A Lower Limb and Power Assist Exoskeleton

Ngoc Khoat Nguyen¹ and Thi Mai Phuong Dao²

¹ School of Automation, University of Electronic Science and Technology of China, Chengdu, Sichuan 611731, China

² College of Electrical and Information Engineering, Hunan University, Changsha, Hunan 410100, China

Abstract

This paper represents the first part of our work in which a successful exoskeleton system has been designed. With this design, the concentration is on effects of compliant human – exoskeleton robot on kinematics and muscle activity during human walking with or without carrying loads. In order to achieve these aims, two control methods are used: kinematic and surface electromyography (sEMG) – based control. In this article, three simulation techniques of sEMG signal are investigated. The obtained results of this work are very useful in designing and testing our actual exoskeleton system.

Keywords: Exoskeleton, Robot, sEMG, Simulation, Control

1. Introduction

In recent decades, exoskeleton robots have been considered and developed purposely to assist the mobility of physically weak persons who are elder, injured and disabled, or extending the strength of humans, especially in the army [4, 6]. A Lower Limb and Power Assist (LLPA) exoskeleton which has been developing in our laboratory is designed mainly for soldiers who always work under hard conditions. A typical LLPA exoskeleton normally consists of a waist holder, a thigh holder, a lower leg holder, two DC motors, two links, a footrest and two force sensors in one leg [6].

In order to control a LLPA exoskeleton system, many control techniques had been taken up [3, 4] in which the sEMG-based control method has attracted a lot of considerations. According to this method, there are plenty of control trends done to reach remarkable achievements. Nevertheless, few of real time sEMG-based exoskeleton systems are available out of laboratories.

The scope of this present research is to explore deeply the simulation techniques of sEMG signals as the first step of our work to evaluate experimental results of real system. Because researches on sEMG signal- based exoskeleton

systems only began a decade ago, models of this signal are still useful for present studies and the future [5, 14]. Most of these models only concentrated on one technique and they were not comprehensive for sEMG signals [3, 13, 15]. This investigation will give three basic models of sEMG signal: physiologically mathematic model, random variable model, and 3-layered volume model. The simulated results are shown clearly to present the survey of sEMG signal which are powerful for LLPA exoskeleton systems.

The second phase of this paper is to analyze two models of sEMG based control scheme of LLPA exoskeleton system: basic and advanced model. These models are evaluated clearly to choose the most suitable control scheme for our system to obtain important design goals of our exoskeleton project as high efficiency and extended application. With the chosen model, we combine a sEMG-based control method with an effective human-exoskeleton robot interaction by using human sensors to measure ankle angles, velocity and acceleration during human walking with or without carrying loads. To implement experiments, we will use an open-circuit respirometer to evaluate human metabolic cost as one of the most important goals of our work.

2. Three sEMG Basic Models

2.1 The Physiologically Mathematic Model

The motor unit in Fig.1 is the smallest activity unit of muscle which is composed by many muscle fibers [8]. The excitability of these muscle fibers through neural control represents a major factor in muscle physiology. To simulate the single fiber potential, we use the volume conduction theory based on the intracellular potential of the fiber [5, 14] which is calculated by (1)

$$e(z)[mV] = 768z^3 \exp(-2z) - 90 \quad (1)$$

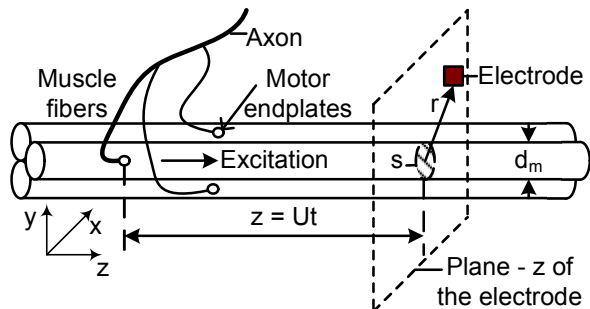


Fig. 1 Motor unit model

where z , in mm , is the axial direction. The transmembrane current is

$$i(z)[mA] = \frac{\sigma_i \pi d_m^2}{4} \frac{d^2 e(z)}{dz^2} \quad (2)$$

where d_m , in μm , is the diameter of the fiber, σ_i is the intracellular conductivity ($\sigma_i = 1.01 Sm^{-1}$ [14]).

A relationship between the axial direction and time domain is expressed in (3)

$$z(U, t)[mm] = Ut \quad (3)$$

where, U , in ms^{-1} , is the propagation velocity of the action potential in the muscle fiber which can be calculated as a function of fiber diameter [5].

$$U(d)[ms^{-1}] = 2.2 + 0.05(d_m - 25) \quad (4)$$

Hence, the single muscle fiber action potential can be yielded by (5)

$$V_{SF_i}[mV] = conv[i(t), w(t)] \quad (5)$$

here $conv$ is symbolic of the convolution and $w(t)$ is the weighting function which can be calculated by [5]. Wang in [15] gave another formula to compute V_{SF_i} in (6).

$$V_{SF_i}[mV] = -\frac{\sigma_i}{4\pi\sigma_m} \int_S \int_{z_{min}}^{z_{max}} \frac{\partial e(z)}{\partial z} \frac{\partial(1/r)}{\partial z} dz \quad (6)$$

where σ_m is the muscle conductivity and r is the distance between the fiber section S and the observation point [5].

Motor unit action potential is obtained in (7) by calculating the total of all the single fiber action potentials

$$V_{MU}[mV] = \sum_{i=1}^N V_{SF_i} \quad (7)$$

with N being the number of muscle fibers which can be defined by [5, 14].

2.2 The Random Variable Model of sEMG

The sEMG signals contain important diagnostic data in both the time and frequency domains. In the time domain, root-mean-square (RMS) value and mean rectified value are two common values in which proportional control of

myoelectric prostheses is typically dependent on the first value of sEMG. In the second domain, the power spectrum density (PSD) is always used as a common value from which measures of median and mean frequency can be extracted to be used for different control goals.

Sometimes, the sEMG signals can be analyzed as a random distribution which is similar to Gaussian signal [13]. Here, the generation of each motor unit action potential is known as a stochastic process of the status of neuromuscular system and the different impulse delay between two consecutive action potentials. This delay can be used as an independent random variable to model each motor unit action potential approximated to an identical distribution. By applying the central limit theorem, the identically distributed and independent motor unit action potential is reasonable to make sEMG as a pseudo-Gaussian distribution with the roughly equal mean of zero as shown in Fig. 2.

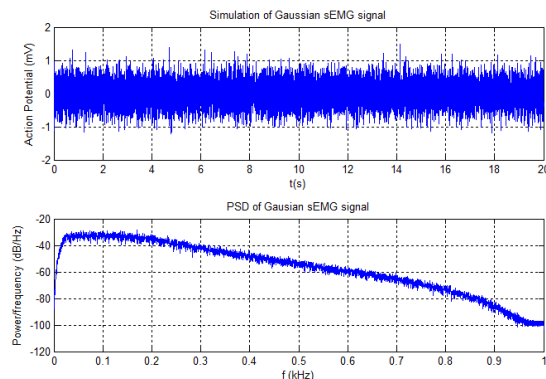


Fig. 2 Simulation of sEMG as a random variable of Gaussian distribution

In order to simulate sEMG signal based on a pseudo-Gaussian distribution, we will use the following formula to calculate the strength of each motor unit action potential:

$$V_{MU_i}[mV] = \frac{1}{\sqrt{r^2 + (z_{max}/2 - i)^2}} \quad (8)$$

where r , in mm , is the distance between the recording site and muscle fiber, z_{max} , in mm , is the length of muscle fiber. Here, we assume that r is a uniformly random variable with a suitable interval from 0.5 to 2 [13].

We also create the sEMG signal by combining a lot of the above motor unit action potentials. To obtain an overall sEMG signal with the representation of time and frequency domains, a bandpass filter with a bandpass filtering of an interval from 20Hz to 200Hz is used in this work.

2.3 A 3-Layered Volume Model for sEMG Signal

Dario Farina and Roberto Merletti in [11] proposed a non-homogeneous (layered) and anisotropic volume conductor

model. By combining with Fansan Zhu in [9], a circuit to simulate sEMG signal based on a 3-layered volume conduction model is presented as shown in Fig. 3.

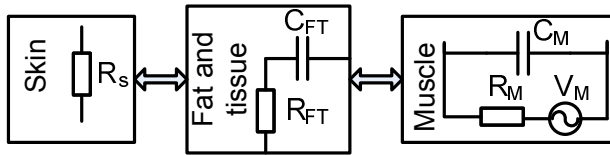


Fig. 3 A 3-layered volume model

This model includes three layers:

- (a) the skin layer: is shown by simple resistors R_s ;
- (b) the fat and tissue layer: is approximated as a low pass filter ($R_{FT}C_{FT}$ filter);
- (c) the muscle fiber layer: is considered as a voltage source with an internal resistor R_M and a natural capacitor C_M of the muscle fiber.

In this model, we assume that values of resistors and capacitors are similar in each area [2, 9]. To obtain the graph of sEMG, a 2-D state space model can be utilized as shown below

$$\vec{X}' = A\vec{X} + B\vec{U} \quad (9)$$

where A , B are state space matrices [7], \vec{U} is the input voltage vector, and \vec{X} is the derivative of output voltage vector. In our work, the intracellular potentials of the fiber given by combining of equations (1) and (3) will be fed to the input voltage vector to create respective sEMG signals. These desired signals can be obtained by measuring output voltages across skin resistors. The simulated values of resistors and capacitors can be found in [2, 9].

2.4 Simulation Results of sEMG Signal

In order to obtain simulation results in time domain, the relationship in (3) will be used. Fig.4 presents simulation results of the intracellular potential and its derivatives in time domain. This potential changes quickly from -90mV up to +40mV and it includes three periods: threshold, depolarization and overshoot. A phase of the membrane named *After Hyperpolarization* which creates instantly a monopolar electrical burst is shown after 1.5ms. This figure also illustrates derivatives of the intracellular potential in which algebraic signs of the first derivative affect the orientation of the dipoles: depolarization with the positive sign and repolarization with the negative sign.

If the fiber diameter is changeable, it is well known to see effects on the intracellular potential as shown in Fig. 5. Here, we assume that the fiber diameter changes from 25 μ m up to 85 μ m [14]. With this change, minimum and

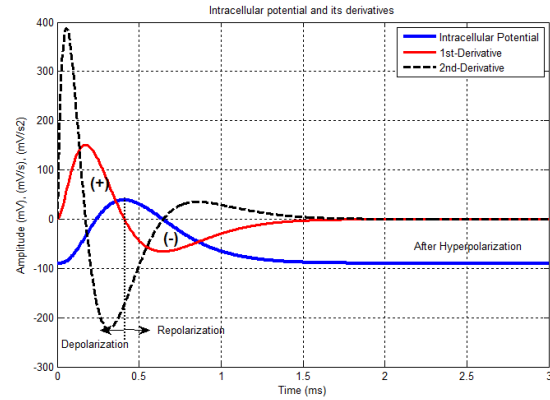


Fig. 4 Simulation results of the intracellular and its derivatives

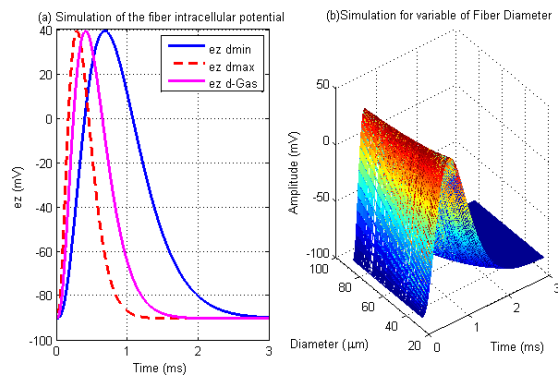


Fig. 5 Effect of fiber diameter on the intracellular potential when fiber diameter changes from $d_{min} = 25\mu\text{m}$ up to $d_{max} = 85\mu\text{m}$.

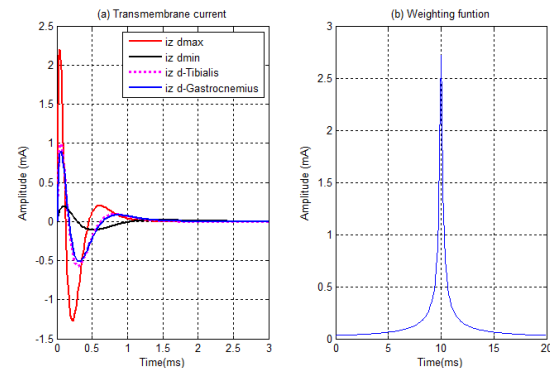


Fig. 6 Simulation of transmembrane current and weighting function. Simulation parameters are: $d_{max} = 85\mu\text{m}$, $d_{min} = 25\mu\text{m}$, $d_{Tibialis anterior} = 57\mu\text{m}$ and $d_{gastrocnemius medialis} = 54\mu\text{m}$ [15].

maximum values of the intracellular potential are not changeable, the corresponding times, however, are variable.

Figure 6 (a) shows the change of transmembrane currents corresponding to the variation of the fiber diameter which belongs to a square relationship. Figure 6 (b) gives the simulation result of a weighting function which is computed by [5].

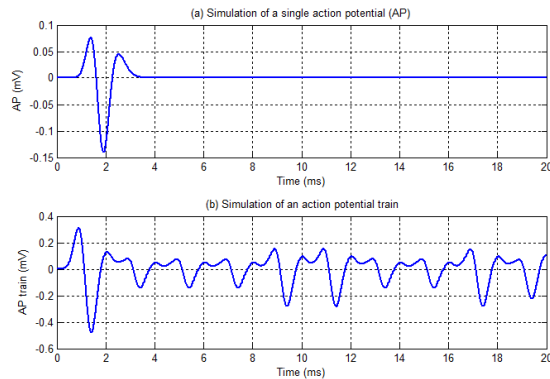


Fig. 7 Simulation of a sEMG signal train.

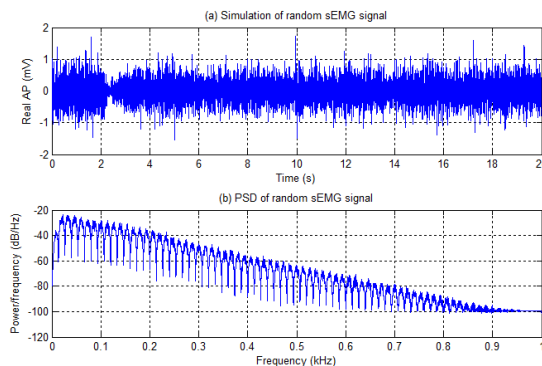


Fig. 8 Simulation of the random sEMG signal.

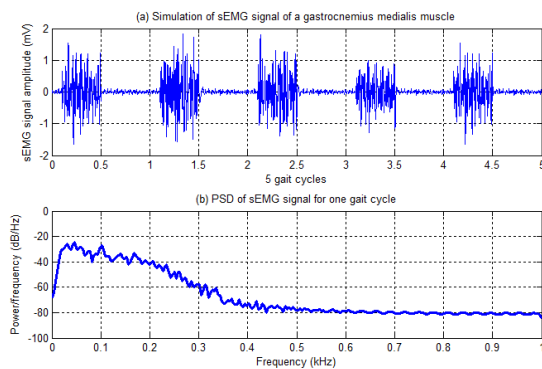


Fig. 9 Simulation results of sEMG signal of the gastrocnemius medialis muscle during gait cycles.

By using algorithms of FFT (*Fast Fourier Transform*) and iFFT (*inverse FFT*), we can compute and simulate the single fiber action potential as shown in Fig. 7. To achieve the superposed sEMG signal of a single fiber motor unit, we combine above motor units at different firing frequencies. In Fig. 7, sEMG signal of measured muscle is well known to reflect the recruitment and firing properties of the discovered motor unit.

According to the second sEMG signal model, simulation results are shown in Fig. 8. Here, conditions of simulation

technique are used similarly with the above Gaussian sEMG signal (Fig. 2) to compare respectively simulated results. Their shapes are clearly close and appropriate to the actual sEMG signal.

With three above models of sEMG signal, aims of simulation are implemented successfully. Figure 9 illustrates the sEMG signal of gastrocnemius medialis muscle which is one of three important muscles in each leg during human walking with five gait cycles that can make a great significance for our exoskeleton system. Simulated parameters are found in [15] and this result is also appropriate for real experiments [15].

3. Analyzing of EMG-Based Control Schemes for LLPA Exoskeleton

In this part, we analyze several control strategies for LLPA exoskeleton based on EMG signal to approach our system. Figure 10 (a) describes a basic control scheme for our work. As shown in this diagram, measured EMG signal is fed to EMG signal processing block to make control signals [1]. Many methods have been investigated successfully to process EMG signal with high-pass filtering, rectification, and then low-pass filtering to obtain a control signal [1, 3, 6]. By combining with the other control blocks as muscle model, gain and controller, needful control signals are fed to LLPA exoskeleton system. These signals are normally used for torque and force of joints to control an exoskeleton robot [7, 10]. Feedback signals that can be used in this model are torque and position signals to implement feedback control for this system [3]. The advantages of this control scheme are simple to construct and implement. Its drawbacks are lower efficiencies and limited applications.

Recent researches have been improved significantly above disadvantages by giving new control schemes [3, 7]. In these systems, interaction between human and exoskeleton is concentrated more efficiently [3, 7, 10] and sensor systems are used for both robot and human as shown in Fig. 10 (b). In this control model, sensors are only used for the robot, such as encoders. Human sensors are applied to measure human parameters as angle, force, velocity, and acceleration of ankle or knee. These parameters are useful to control an exoskeleton for other goals of stroke patient rehabilitation [12] or extending the strength of humans [3]. These systems can be called as exoskeleton robot intelligent systems.

In order to apply a model for our work, besides above sensors, an open-circuit respirometer is used to measure oxygen consumption and carbon dioxide production to estimate human metabolic cost during walking with or

without LLPA exoskeleton and with carrying military loads of 20 kg, 40 kg, and 55 kg. According to the aim of our exoskeleton system, the most important design tasks are to reduce the metabolic cost of locomotion and minimize the power requirements of assisted robot. With these tasks, sEMG signal-based control is able to achieve lower metabolic cost than those under kinematic control.

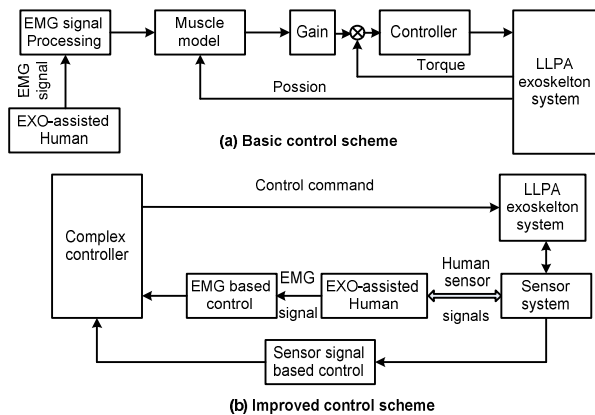


Fig. 10 Diagram of EMG-based control schemes.

4. Conclusions

In this paper, sEMG signal simulation techniques and control schemes of EMG-based LLPA exoskeleton system are presented. Although simulation techniques of sEMG signal are vast, three models of them are discussed as the most popular approaches. The first is the most basic, the second is the most easy, and the third is the most exact to simulate sEMG signal for goals of study and evaluation of simulated models with real systems. The other part of this paper explains two general models of EMG-based control algorithm for a LLPA exoskeleton in which the second one is applied for our work as an exoskeleton robot intelligent system. In the near future, we will perform this model and compare with real system to reach successfully given tasks in the exoskeleton project in our laboratory.

Acknowledgments

The authors would like to thank members of PRMI laboratory for assistance to implement this exoskeleton project.

References

[1] A. Salman, J. Iqbal, U. Izhar, U.S. Khan, and N. Rashid, "Optimized circuit for EMG signal processing", *2012 International Conference on Robotics and Artificial Intelligence (ICRAI)*, 2012. 208-213.
 [2] A.K. Mahablagini, K. Ahmed and F.Schlereth, "A novel approach for simulation, measurement and representation of surface EMG signals", *Conference Record of the Forty Fifth Asilomar Conference*

on. ASILOMAR 2011: Signals, Systems and Computers, 2011. 476-480.
 [3] Ram Murat Singh and S. Chatterji, "Trends and challenges in EMG based control scheme of exoskeleton robots - a review." *International Journal of Scientific and Engineering Research*, 3(8), 2012: 1-8.
 [4] Gregory S. Sawicki and Daniel P. Ferris, "Mechanics and energetics of incline walking with robotic ankle exoskeletons", *Journal of Experimental Biology*, 212(1), 2009: 32-41.
 [5] J.Duchene & J.-Y.Hogrel, "A model of EMG generation", *Biomedical Engineering, IEEE Transaction on*, 47(2), 2000: 192-201.
 [6] Kazuo Kiguchi and Y. Imada, "EMG-based control for lower-limb power-assist exoskeletons", *IEEE Workshop on. RIIS '09: Robotic Intelligence in Informationally Structured Space*, 2009. 19-24.
 [7] H.He and K. Kiguchi, "A study on EMG-based control of exoskeleton robots for human lower-limb motion assist", *6th International Special Topic Conference on. ITAB 2007: Information Technology Application in Biomedicine*, 2007. 292-295.
 [8] Konral, Peter. *The ABC of EMG. A Practical Introduction to Kinesiological Electromyography*, 2005.
 [9] Fansan Zhu and N. W. Levin, "An electrical resistivity model of segmental body composition using bioimpedance analysis", *Proceedings of the 25th Annual International Conference of the IEEE. Engineering in Medicine and Biology Society*, 2003, 2003. 2679-2682.
 [10] D.P. Ferris and C.L. Lewis, "Robotic lower limb exoskeleton using proportional myoelectric control", *Annual International Conference of the IEEE. Engineering in Medicine and Biology Society*, 2009. 2119-2124.
 [11] Dario Farina and Roberto. Merletti, "A novel approach for precise simulation of the EMG signal detected by surface electrodes", *Biomedical Engineering, IEEE Transactions on*, 2001: 637-646.
 [12] O. Unluhisarcikli, M. Pietrusinski, B. Weinberg, P. Bonato, and C. Mavroidis, "Design and control of a robotic lower extremity exoskeleton for gait rehabilitation", *2011 IEEE/RSJ International Conference on. Intelligent Robots and Systems (IROS)*, 2011. 4893-4898.
 [13] S. Patrick, J. Meklenburg, S. Jung, Y. Mendelson, and E.A. Clancy, "An electromyogram simulator for myoelectric prosthesis testing", *Proceedings of the 2010 IEEE 36th Annual Northeast. Bioengineering Conference*, 2010.
 [14] Sanjeev D.Nandedkar, E.V. Stalberg and Donald B.Sanders, "Simulation techniques in electromyography", *Biomedical Engineering, IEEE Transaction on* 32, no. 10 (1985): 775-785.
 [15] W. Wang, A. De. Stefano, and R.Allen, "A simulation model of the surface EMG signal for analysis of muscle activity during the gait cycle", *Computer in Biology and Medicine*, 36(6), 2006: 601-618.



Ngoc Khoat Nguyen received Msc degree in *Automation and Control* at Hanoi University of Science and Technology, in 2009. He is working as a Lecturer at Electric Power University in Hanoi, Vietnam. He is now doing PhD in the field of Automation at University of Electronic Science and Technology of China, Chengdu, Sichuan, China. His research interests include modeling and application of sEMG signal, control motor and robot.



Thi Mai Phuong Dao received Msc degree in *Automation and Control* at Hanoi University of Science and Technology, in 2010. She is working as a Lecturer at Hanoi University of Industry in Hanoi, Vietnam. She is now doing PhD in the field of Automation at Hunan University, Changsha, Hunan, China. Her research interests include modeling and experiment of sEMG signal, control theory and application.